Journal of Structural Engineering & Applied Mechanics (2022) 5(4):277-288
DOI 10.31462/jseam.2022.04277288

RESEARCH ARTICLE

# Free vibration analysis of a porous functionally graded beam using higher-order shear deformation theory

Gökhan Adıyaman*

Karadeniz Technical University, Faculty of Engineering, Department of Civil Engineering, Trabzon, Turkiye

## Article History

Received 30 July 2022
Accepted 6 December 2022

## Keywords

FGM
HSDT
Finite element method

## Abstract

This study considers free vibration analysis of a porous functionally graded (FG) beam using a higher-order shear deformation theory (HSDT). The change in the material properties is described by a power law. The porosity distribution functions, one for even cases and two for uneven cases, are considered in the problem. The governing equations are derived utilizing Lagrange's principle. The solution to the problem is carried out using FEM with a three-node and 12-DOF element. Dimensionless natural frequencies obtained in the present study are compared to those reported in four studies from the literature for validation purposes. The effect of material properties, porosity, and boundary conditions on the dimensionless neutral frequencies and mode shapes are investigated with the help of a parametric study.

## 1. Introduction

Composite material is an emerging idea to combine different materials as layered media to achieve better material properties. However, this layered structure causes stress and temperature discontinuities in the material. A new material named functionally graded (FG) was proposed to overcome this problem in the 1980s. In FG materials, the properties in the material gradually change from one material to another depending on a function. Due to their superior properties, they have been used in many engineering applications, especially in aerospace, biomedical, and automotive.

Ceramics and metal are two materials that are generally used in the production of FG materials. However, voids and cavities, which are frequently generated in the ceramic phase rather than the metallic one, are formed in the FG materials in the fabrication process. In recent years, determining the effect of this porosity on the mechanical behavior of the FG beam has been the focus of researchers. Some of the studies using the analytical solution in this area are summarized below.

Chen et al. [7] presented the buckling and bending analysis of an FG porous beam based on the Timoshenko beam theory. The free vibration problem of an imperfect FG beam based on the Timoshenko beam theory was studied by Wattanasakulpong and Chaikittiratana [8]. Ebrahimi et al. [9] investigated the thermo-mechanical vibration analysis of a porous Euler FG beam using a Navier-type solution. The analytical solution for bending, free vibration, and buckling problems of a porous FG beam considering both shear

* Corresponding author (gadiyaman@ktu.edu.tr)

eISSN 2630-5763 

deformations and thickness stretching was studied by Atmane et al. [10]. Al Rjoub and Hamad [11] considered the free vibration of porous Euler-Bernoulli and Timoshenko FG beams using the transfer matrix method. Free vibration and buckling of a porous FG beam reinforced by graphene platelets were investigated by Kitipornchai et. al [12] using the Timoshenko beam theory and Ritz method. Hadji et al. [3] studied the analytical solution for bending and free vibration problems of a porous FG microbeam. The bending analysis of a porous Timoshenko FG beam was presented by Thi et al. [13]. Tang et al. [14] developed a unified nonlocal strain gradient beam model with the thickness effect to investigate the static bending behavior of micro/nano-scale porous FG beams. The free vibration analysis of a porous FG beam was investigated by Taskın and Demirhan [15] using the Navier approach. Harsha et al. [3] considered the effect of the porosity and axial loading on the buckling and free vibration of a porous FG beam using the Ritz method. The buckling characteristics of porous sandwich FG beams were investigated by Drikvand et al. [16] with the help of the differential transform method. Nguyen et al. [17] presented a new shear deformation theory for the bending, buckling, and vibration behaviors of porous FG beams.

Finite element is one of the most used numeric methods in the analysis of the porous FG beams. Fouda et al. [18] studied the bending, buckling, and vibration of a porous Euler-Bernoulli FG beam utilizing the finite element method (FEM) using a two-node element. The forced vibration analysis of porous FG deep beam under dynamical loading was investigated by Akbas [19] using a 12-node plane element. Wu et al. [20] introduced a FEM analysis framework for free and forced vibration of porous both Euler-Bernoulli and Timoshenko FG beams using a 2-node 6-degree of freedom (DOF) element. The same authors [21] used a non-deterministic approach to solve the same problem. The mechanical behaviors of porous FG nanobeams for bending were investigated by Hamed et al. [22] using a 2-node 6-DOF element. Karamanli and Vo [23] studied the size-dependent responses of porous FG micro-beams using a quasi-3D theory and the modified strain gradient theory. The bending analysis of a porous FG beam using a two-node 4-DOF finite element is investigated by Zghal et al. [24]. Alnujaie et al. [25] considered the forced vibration analysis of a porous FG thick beam using a 12-node plane element.

According to the studies mentioned above and the author's knowledge, the higher-order shear deformation theory was not considered in the formulation of the FEM solution of porous FG beams. Therefore, the errors in the solutions rise above the acceptable level in the case of short beams. This paper investigates FEM analysis of the free vibration of porous FG beams using a higher-order shear deformation theory. Three different porosity distributions, one even and two uneven, are considered in the study. A tree-node 12-DOF finite element is used in the solution. The present study is verified by using four studies from the literature. A parametric study is carried out to investigate dimensionless neutral frequencies and mode shapes for various material properties, porosities, and boundary conditions.

## 2. Theory and formulation for free vibration of an FG beam

### 2.1. Material properties of an FG porous beam

In this study, a functionally graded (FG) porous beam of length $L$, thickness $h$, and width $b$ is considered. The top of the beam is loaded by a uniformly distributed load of magnitude $q_0$ in the $z$-direction at $y = 0$. The material properties of the beam such as Young's modulus $E(z)$, the mass density $\rho(z)$, and Poisson's ratio $\nu(z)$ vary through the thickness ($z$-axis) depending on a power law function. In addition, it is assumed that the porosity in the beam averagely affects the material properties as given,

$$P(z) = P_b + (P_t - P_b)\left(\frac{z}{h} + \frac{1}{2}\right)^p - \frac{e}{2} f_e(z)(P_t + P_b) \tag{1}$$

where $P_b$ and $P_t$ are the values of any material property at the bottom and at the top of the beam, respectively; $p$ is named the power law index and controls the variation in the material property; $e$ refers to the porosity coefficient which presents the ratio of the void volume to the total volume ($0 < e < 1$), $f_e(z)$ is a function that shows the distribution of the porosities through the thickness. Three $f_e(z)$ are used in this study.

$$f_{e,1}(z) = 1, \qquad f_{e,2}(z) = 1 - \frac{2|z|}{h}, \qquad f_{e,3}(z) = sin\left(\frac{|z|}{h}\pi\right) \tag{2-4}$$

The distribution of the porosity through the cross-sections corresponding to three distribution functions, namely Even (1), Uneven-I (2), and Uneven-II (3), is given in Fig.2. For Even, the porosities are uniformly distributed along the beam cross-section, whereas the porosities are spread mostly around the middle and the corners of the cross-section for Uneven-I and Uneven-II, respectively. The variation of Young's modulus $E$ in Even and Uneven-II for various $p$ and $e$ are given in Fig 3. The observation of the figure shows that when porosity goes to zero ($z \to 0$ for uneven-II), $E$ approaches the value in perfect cross-section ($e = 0$).

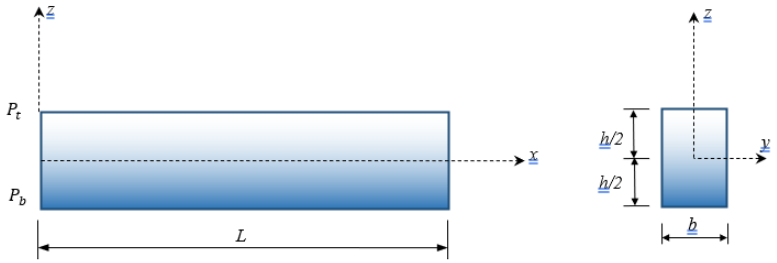


Fig. 1. The geometry and loading of the FG porous beam

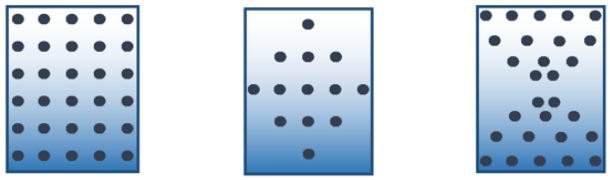

(a) Even (b) Uneven-I (c) Uneven-II

Fig. 2. The beam cross-sections for three distribution functions

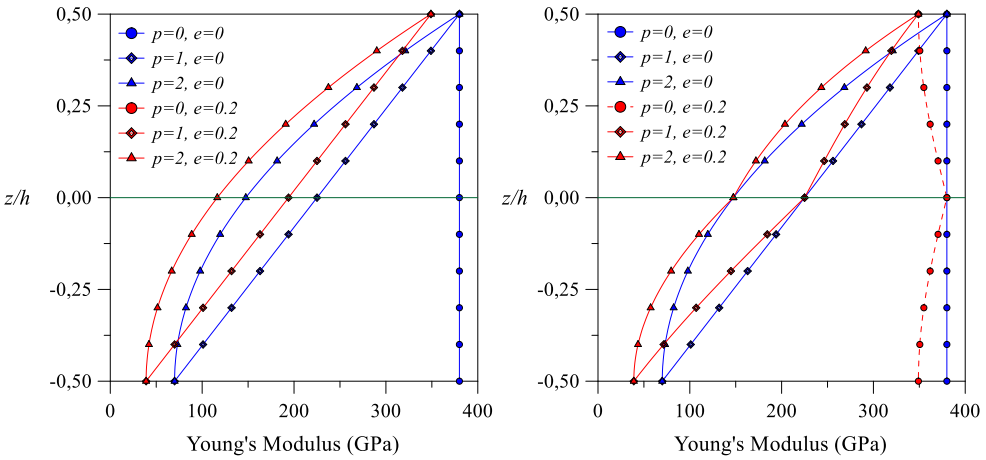


Fig. 3. The variation of $E$ with $p$ and $e$ for (a) even and (b) uneven-II

## 2.2. Mathematical formulation

The displacement field of a beam according to the exponentially higher order shear deformation theory can be expressed as follows [2]:

$$u(x,z) = u_0(x) - z\phi + f(z)\beta, \qquad w(x) = w_0(x), \qquad f(z) = ze^{-2(z/h)^2} \tag{5-7}$$

where *u* and *w* are the displacements in the *x*- and *z*-axis, respectively; $u_0$ and $w_0$ represent the displacements at the neutral axis ($z = 0$); $\phi$ and $\beta$ imply the terms related to rotations; and *f*(*z*) is a function that reflects the higher-order deformation at the cross-section and is given in Karama et al. [1]. Axial normal and transverse shear stains corresponding to the displacement field can be expressed as given below:

$$\varepsilon_{xx} = \frac{du_0(x)}{dz} - z\frac{d\phi}{dx} + f(z)\frac{d\beta}{dx}, \qquad \gamma_{xz} = \frac{dw_0(x)}{dx} - \phi + \frac{df(z)}{dz}\beta \tag{8-9}$$

Since the transverse normal strain is neglected, the constitutive equations can be expressed as

$$\sigma_{xx} = E(z)\varepsilon_{xx}, \qquad \tau_{xz} = G(z)\gamma_{xz} \tag{10-11}$$

where $E$ and $G$ are the Young's and shear modulus of the material, respectively.

A three-node higher-order beam element of length $L_e$ with 12 DOFs shown in Fig. 4 can be used in the finite element solution. The displacement field can be expressed in terms of generalized nodal displacements as follows:

$$u_0(x) = \sum_{i=1}^{3}\psi_i(x)u_i, \quad w_0(x) = \sum_{i=1}^{3}\psi_i(x)w_i, \quad \phi_0(x) = \sum_{i=1}^{3}\psi_i(x)\phi_i, \quad \beta_0(x) = \sum_{i=1}^{3}\psi_i(x)\beta_i, \tag{12-15}$$

where $\psi_i$ ($i$=1,2,3) presents shape functions and can be found by applying quadratic interpolation.

$$\psi_1 = (1-\frac{x}{L_e})(1-2\frac{x}{L_e}), \quad \psi_2 = 4\frac{x}{L_e}(1-\frac{x}{L_e}), \quad \psi_3 = -\frac{x}{L_e}(1-2\frac{x}{L_e}) \tag{16-18}$$

The strain ($U$) and kinetic ($T$) energy of a beam can be expressed as follows:

$$U = \int_0^L\int_A(\sigma_{xx}\varepsilon_{xx} + \tau_{xz}\gamma_{xz})dAdx, \qquad T = \int_0^L\int_A\rho(z)(\dot{u}^2 + \dot{w}^2)dAdx \tag{19-20}$$

where dot denotes the derivative with respect to time Letting $L = T - U$, the governing equations of the motion can be obtained with the help of Lagrange's defined as follows:

$$\frac{d}{dt}\left(\frac{\partial L}{\partial \dot{q}_i}\right) - \frac{\partial L}{\partial q_i} = 0 \tag{21}$$

where $q_i$ ($i$=1,2,3) in Eq. (21) presents generalized nodal displacements corresponding to $u_i$, $w_i$, $\phi_i$ and $\beta_i$ which are unknowns of the equations. Substituting necessary equations into Eq. (21), the equation of motion for one element can be obtained as

$$\mathbf{m}\ddot{\boldsymbol{u}} + \boldsymbol{ku} = \mathbf{0} \tag{22}$$

where $\boldsymbol{m}$ and $\boldsymbol{k}$ present element mass and stiffness matrix, respectively. For a beam of length $L$ composed of $N$ elements, the following equation of motion can be written:

$$\mathbf{M}\ddot{\boldsymbol{U}} + \boldsymbol{KU} = \mathbf{0} \tag{23}$$

where $\boldsymbol{M}$ and $\boldsymbol{K}$ are the global mass and stiffness matrix, respectively, $\boldsymbol{U}$ shows the vector of global unknown nodal displacements. If the solution of Eq. (23) is sought as $U = U_0 e^{i\omega t}$, an eigenvalue and eigenvector problem can be obtained as follows:

$$(\boldsymbol{K} - \omega^2 \boldsymbol{M})\boldsymbol{U_0} = 0 \tag{24}$$

where $\omega$ denotes the natural frequencies of the beam.

## 3. Numerical results and discussion

In the numerical results, it is assumed that the bottom of the beam is metal-rich whereas the top of the beam is ceramic-rich. Material properties used in the solutions are given in Table 1. The results are obtained for three boundary conditions of the beam namely simple supported (SS), clamped (CC), and cantilever (CF). Note that the natural frequencies in the results are given normalized as follows:

$$\bar{\omega} = \frac{\omega L^2}{h}\sqrt{\frac{\rho_m}{E_m}} \tag{25}$$

where subscript $m$ donates properties related to metal. Table 2 shows the results of a convergence analysis carried out for all porosity functions and boundary conditions to determine the number of elements in the solutions. As can be seen from the table, natural frequencies converge if the number of elements is increased, and 50 elements provide enough relative error of less than 0.01% in any case.

The verification of the frequencies obtained in the present study with the frequencies reported in Hadji et al. [3] for various $L/h$ and porosity types is given in Table 2. Hadji et al. [3] used a Navier-type analytical solution based on a higher-order shear model. The effect of solution methods is taken into account, especially deep beams. Since a numerical solution method (FEM) is used in the present study, obtained results in the present study are slightly smaller compared to analytical results. It can be observed from the table the maximum relative difference between present and reported frequencies is less than 0.015 and the differences decrease for increasing $L/h$. In Table 4, another verification of the frequencies obtained in the study in the case of the perfect cross-section with the frequencies given in Kahya and Turan [4], Nguyen et al. [5], and Vo et al. [6] for various $p$ and boundary conditions are given. In their studies, Kahya and Turan [4] used FEM based on the first-order shear deformation theory, Nguyen et al. [5] used an analytical solution method based on higher-order shear deformation theory and Vo et al. [6] used FEM based on a higher-order shear deformation theory for non-porous beams. Examination of the table shows that frequencies obtained in the present study are only slightly different from the frequencies reported in the literature, especially with the ones that used higher-order shear deformation theory because of the similarity in theories.

Table 1. Material properties used in the solutions

| Material | $E\ (GPa)$ | $\upsilon$ | $\rho\ \left(\frac{kg}{m^3}\right)$ |
|---|---|---|---|
| Metal | 70 | 0.3 | 2702 |
| Ceramic | 380 | 0.3 | 3960 |

Table 2. Convergence analysis for different porosity functions and boundary conditions ($L/h = 5$, $p = 1$, $e = 0.1$)

| Number of elements | Even | | | Uneven-I | | | Uneven-II | | |
|---|---|---|---|---|---|---|---|---|---|
| | SS | CC | CF | SS | CC | CF | SS | CC | CF |
| 2 | 4.0373 | 9.7208 | 1.4579 | 4.2531 | 10.0837 | 1.5377 | 4.0974 | 9.8982 | 1.4775 |
| 5 | 3.8892 | 7.8546 | 1.4324 | 4.1017 | 8.2167 | 1.5116 | 3.9452 | 7.9865 | 1.4514 |
| 10 | 3.8839 | 7.7970 | 1.4314 | 4.0963 | 8.1579 | 1.5106 | 3.9397 | 7.9283 | 1.4504 |
| 15 | 3.8836 | 7.7930 | 1.4314 | 4.0960 | 8.1537 | 1.5105 | 3.9394 | 7.9243 | 1.4504 |
| 20 | 3.8835 | 7.7922 | | 4.0959 | 8.1528 | 1.5105 | 3.9393 | 7.9235 | |
| 30 | 3.8835 | 7.7919 | | 4.0959 | 8.1525 | | 3.9393 | 7.9232 | |
| 50 | | 7.7918 | | | 8.1524 | | | 7.9232 | |
| 75 | | 7.7918 | | | 8.1524 | | | | |

Table 3. The verification of the frequencies obtained in the present study with the frequencies reported in Hadji et al. [3] ($p = 2$)

| $L/h$ | Study | Even | | | Uneven-I | | |
|---|---|---|---|---|---|---|---|
| | | $e = 0$ | $e = 0.1$ | $e = 0.2$ | $e = 0$ | $e = 0.1$ | $e = 0.2$ |
| 5 | Hadji et al. [3] | 3.6264 | 3.4418 | 3.1489 | 3.6264 | 3.6069 | 3.5785 |
| | Present | 3.5970 | 3.4050 | 3.1023 | 3.5970 | 3.5736 | 3.5405 |
| 20 | Hadji et al. [3] | 3.8361 | 3.6335 | 3.3123 | 3.8361 | 3.8226 | 3.8004 |
| | Present | 3.8341 | 3.6308 | 3.3090 | 3.8341 | 3.8201 | 3.7975 |

Table 4. The verification of the frequencies obtained in the present study with the frequencies reported in Kahya and Turan [4], Nguyen et al. [5], and Vo et al. [6] ($L/h = 5$)

| BC | Study | $p = 0$ | $p = 0.5$ | $p = 1$ | $p = 2$ | $p = 5$ | $p = 10$ |
|---|---|---|---|---|---|---|---|
| SS | Kahya and Turan [4] | 5.2219 | 4.4692 | 4.0496 | 3.6936 | 3.4881 | 3.3643 |
| | Nguyen et al. [5] | 5.1528 | 4.4102 | 3.9904 | 3.6264 | 3.4009 | 3.2815 |
| | Vo et al. [6] | 5.1528 | 4.4019 | 3.9716 | 3.5979 | 3.3743 | 3.2653 |
| | Present | 5.1532 | 4.4016 | 3.9710 | 3.5970 | 3.3725 | 3.2644 |
| CC | Kahya and Turan [4] | 10.0864 | 8.7547 | 7.9841 | 7.2715 | 6.7148 | 6.3741 |
| | Nguyen et al. [5] | 10.0726 | 8.7463 | 7.9518 | 7.1776 | 6.4929 | 6.1658 |
| | Vo et al. [6] | 10.0678 | 8.7457 | 7.9522 | 7.1801 | 6.4961 | 6.1662 |
| | Present | 10.0321 | 8.7114 | 7.9200 | 7.1496 | 6.4626 | 6.1355 |
| CF | Kahya and Turan [4] | 1.9077 | 1.6286 | 1.4739 | 1.3446 | 1.2751 | 1.2636 |
| | Nguyen et al. [5] | 1.8957 | 1.6182 | 1.4636 | 1.3328 | 1.2594 | 1.2187 |
| | Vo et al. [6] | 1.8952 | 1.6180 | 1.4633 | 1.3326 | 1.2592 | 1.2184 |
| | Present | 1.8948 | 1.6176 | 1.4629 | 1.3322 | 1.2586 | 1.2178 |

Table 5. The neutral frequencies of a beam for various porosity types, boundary conditions, $e$ and $p$ ($L/h = 5$)

| Type | BC | $e$ | $p = 0$ | $p = 0.5$ | $p = 1$ | $p = 2$ | $p = 5$ | $p = 10$ |
|---|---|---|---|---|---|---|---|---|
| Even | SS | 0 | 5.1532 | 4.4016 | 3.9710 | 3.5970 | 3.3725 | 3.2644 |
| | | 0.1 | 5.2223 | 4.3934 | 3.8835 | 3.4050 | 3.1083 | 3.0028 |
| | | 0.2 | 5.3047 | 4.3798 | 3.7577 | 3.1023 | 2.6403 | 2.5273 |
| | | 0.3 | 5.4040 | 4.3573 | 3.5658 | 2.5572 | 1.4574 | 1.1164 |
| | CC | 0 | 10.0321 | 8.7114 | 7.9200 | 7.1496 | 6.4626 | 6.1355 |
| | | 0.1 | 10.1621 | 8.7170 | 7.7918 | 6.8439 | 6.0019 | 5.6231 |
| | | 0.2 | 10.3225 | 8.7178 | 7.6032 | 6.3561 | 5.2216 | 4.7437 |
| | | 0.3 | 10.5158 | 8.7094 | 7.3061 | 5.4349 | 3.2140 | 2.3636 |
| | CF | 0 | 1.8948 | 1.6176 | 1.4629 | 1.3322 | 1.2586 | 1.2178 |
| | | 0.1 | 1.9203 | 1.6147 | 1.4313 | 1.2630 | 1.1649 | 1.1266 |
| | | 0.2 | 1.9506 | 1.6098 | 1.3858 | 1.1533 | 0.9963 | 0.9592 |
| | | 0.3 | 1.9872 | 1.6016 | 1.3162 | 0.9539 | 0.5559 | 0.4339 |
| Uneven-I | SS | 0 | 5.1532 | 4.4016 | 3.9710 | 3.5970 | 3.3725 | 3.2644 |
| | | 0.1 | 5.2184 | 4.4429 | 3.9850 | 3.5737 | 3.3193 | 3.2112 |
| | | 0.2 | 5.2888 | 4.4872 | 3.9978 | 3.5405 | 3.2417 | 3.1252 |
| | | 0.3 | 5.3644 | 4.5345 | 4.0087 | 3.4939 | 3.1251 | 2.9710 |
| | CC | 0 | 10.0321 | 8.7114 | 7.9200 | 7.1496 | 6.4626 | 6.1355 |
| | | 0.1 | 10.1273 | 8.7717 | 7.9324 | 7.0887 | 6.2970 | 5.9242 |
| | | 0.2 | 10.2342 | 8.8350 | 7.9412 | 7.0081 | 6.0665 | 5.6045 |
| | | 0.3 | 10.3482 | 8.9015 | 7.9447 | 6.9009 | 5.7300 | 5.0676 |
| | CF | 0 | 1.8948 | 1.6176 | 1.4629 | 1.3322 | 1.2586 | 1.2178 |
| | | 0.1 | 1.9202 | 1.6342 | 1.4699 | 1.3264 | 1.2445 | 1.2055 |
| | | 0.2 | 1.9475 | 1.6521 | 1.4767 | 1.3173 | 1.2230 | 1.1844 |
| | | 0.3 | 1.9769 | 1.6713 | 1.4830 | 1.3038 | 1.1895 | 1.1455 |
| Uneven-II | SS | 0 | 5.1532 | 4.4016 | 3.9710 | 3.5970 | 3.3725 | 3.2644 |
| | | 0.1 | 5.1633 | 4.3512 | 3.8633 | 3.4184 | 3.1517 | 3.0452 |
| | | 0.2 | 5.1747 | 4.2911 | 3.7297 | 3.1828 | 2.8423 | 2.7376 |
| | | 0.3 | 5.1872 | 4.2184 | 3.5602 | 2.8568 | 2.3646 | 2.2533 |
| | CC | 0 | 10.0321 | 8.7114 | 7.9200 | 7.1496 | 6.4626 | 6.1355 |
| | | 0.1 | 10.0749 | 8.6571 | 7.7698 | 6.8867 | 6.1421 | 5.8047 |
| | | 0.2 | 10.1269 | 8.5875 | 7.5747 | 6.5227 | 5.6788 | 5.3373 |
| | | 0.3 | 10.1832 | 8.4973 | 7.3142 | 5.9865 | 4.9161 | 4.5760 |
| | CF | 0 | 1.8948 | 1.6176 | 1.4629 | 1.3322 | 1.2586 | 1.2178 |
| | | 0.1 | 1.8973 | 1.5978 | 1.4222 | 1.2654 | 1.1760 | 1.1356 |
| | | 0.2 | 1.9001 | 1.5743 | 1.3720 | 1.1777 | 1.0607 | 1.0209 |
| | | 0.3 | 1.9032 | 1.5461 | 1.3086 | 1.0569 | 0.8832 | 0.8411 |

Table 6. The neutral frequencies of a beam in case of Even cross-section for various porosity types, $e$ and $p$ $(L/h = 20)$

| Type | BC | $e$ | $p = 0$ | $p = 0.5$ | $p = 1$ | $p = 2$ | $p = 5$ | $p = 10$ |
|---|---|---|---|---|---|---|---|---|
| Even | SS | 0 | 5.4603 | 4.6505 | 4.2037 | 3.8341 | 3.6464 | 3.5377 |
| | | 0.1 | 5.5341 | 4.6405 | 4.1101 | 3.6308 | 3.3746 | 3.2789 |
| | | 0.2 | 5.6215 | 4.6245 | 3.9756 | 3.3090 | 2.8814 | 2.7986 |
| | | 0.3 | 5.7267 | 4.5986 | 3.7707 | 2.7271 | 1.5907 | 1.2532 |
| | CC | 0 | 12.2213 | 10.4258 | 9.4300 | 8.5960 | 8.1419 | 7.8833 |
| | | 0.1 | 12.3861 | 10.4057 | 9.2248 | 8.1482 | 7.5391 | 7.3006 |
| | | 0.2 | 12.5817 | 10.3729 | 8.9295 | 7.4384 | 6.4505 | 6.2276 |
| | | 0.3 | 12.8174 | 10.3189 | 8.4787 | 6.1494 | 3.5959 | 2.8204 |
| | CF | 0 | 1.9496 | 1.6603 | 1.5010 | 1.3696 | 1.3033 | 1.2645 |
| | | 0.1 | 1.9759 | 1.6567 | 1.4677 | 1.2971 | 1.2066 | 1.1725 |
| | | 0.2 | 2.0071 | 1.6510 | 1.4197 | 1.1823 | 1.0307 | 1.0016 |
| | | 0.3 | 2.0447 | 1.6417 | 1.3465 | 0.9745 | 0.5693 | 0.4493 |
| Uneven-I | SS | 0 | 5.4603 | 4.6505 | 4.2037 | 3.8341 | 3.6464 | 3.5377 |
| | | 0.1 | 5.5369 | 4.7010 | 4.2261 | 3.8201 | 3.6147 | 3.5169 |
| | | 0.2 | 5.6193 | 4.7553 | 4.2483 | 3.7975 | 3.5651 | 3.4800 |
| | | 0.3 | 5.7082 | 4.8140 | 4.2697 | 3.7626 | 3.4873 | 3.4143 |
| | CC | 0 | 12.2213 | 10.4258 | 9.4300 | 8.5960 | 8.1419 | 7.8833 |
| | | 0.1 | 12.3887 | 10.5359 | 9.4778 | 8.5622 | 8.0598 | 7.8166 |
| | | 0.2 | 12.5689 | 10.6545 | 9.5250 | 8.5087 | 7.9334 | 7.7015 |
| | | 0.3 | 12.7632 | 10.7823 | 9.5703 | 8.4272 | 7.7350 | 7.4879 |
| | CF | 0 | 1.9496 | 1.6603 | 1.5010 | 1.3696 | 1.3033 | 1.2645 |
| | | 0.1 | 1.9770 | 1.6784 | 1.5092 | 1.3648 | 1.2925 | 1.2577 |
| | | 0.2 | 2.0065 | 1.6980 | 1.5172 | 1.3570 | 1.2754 | 1.2455 |
| | | 0.3 | 2.0384 | 1.7191 | 1.5251 | 1.3448 | 1.2486 | 1.2240 |
| Uneven-II | SS | 0 | 5.4603 | 4.6505 | 4.2037 | 3.8341 | 3.6464 | 3.5377 |
| | | 0.1 | 5.4644 | 4.5891 | 4.0812 | 3.6347 | 3.3986 | 3.2914 |
| | | 0.2 | 5.4690 | 4.5169 | 3.9311 | 3.3751 | 3.0551 | 2.9493 |
| | | 0.3 | 5.4741 | 4.4310 | 3.7431 | 3.0202 | 2.5317 | 2.4176 |
| | CC | 0 | 12.2213 | 10.4258 | 9.4300 | 8.5960 | 8.1419 | 7.8833 |
| | | 0.1 | 12.2340 | 10.2934 | 9.1623 | 8.1594 | 7.6019 | 7.3459 |
| | | 0.2 | 12.2482 | 10.1374 | 8.8336 | 7.5886 | 6.8505 | 6.5979 |
| | | 0.3 | 12.2638 | 9.9509 | 8.4198 | 6.8039 | 5.6976 | 5.4297 |
| | CF | 0 | 1.9496 | 1.6603 | 1.5010 | 1.3696 | 1.3033 | 1.2645 |
| | | 0.1 | 1.9509 | 1.6383 | 1.4572 | 1.2983 | 1.2147 | 1.1764 |
| | | 0.2 | 1.9524 | 1.6124 | 1.4035 | 1.2055 | 1.0919 | 1.0541 |
| | | 0.3 | 1.9541 | 1.5816 | 1.3363 | 1.0787 | 0.9048 | 0.8640 |

The neutral frequencies of a beam for various porosity types, boundary conditions, porosity coefficient, and power law index in the case of $L/h = 5$ and $L/h = 20$ are given in Tables 5 and 6, respectively. The above-given tables show that the frequencies increase if $e$ increases for $p = 0$ whereas the increase in $e$ results in a decrease in frequencies for $p > 0$. Both density and shear modules change according to Eq. (1). However, the relative change in density is larger compared to the relative change in shear modulus about $p = 0$ if the porosity increases. Since global stiffness matrix **K** includes shear modulus and global mass matrix **M** includes density, from the investigation of Eq. (24), natural frequencies increases if porosity increases. However, the relative change in shear modulus exceeds the relative change in density for $p \geq 0.5$ and the frequencies increase with increasing porosity. If $L/h$ increases, the neutral frequencies also increase. The change in the frequencies for increasing porosity is maximum for the Even type whereas it is minimum for Uneven-I.

Fig. 5a and 5b show the frequencies for $L/h$ ratio and power law index, respectively, for various porosity coefficients. As can be seen from the figures, the frequencies approach asymptotically to a finite value if $L/h \to \infty$ and $p \to \infty$. Increasing $L/h$ results in an increase in the frequencies, but if $p$ increases, the frequencies decrease. As the porosity increases, the relative change at the frequencies becomes smaller with increasing $L/h$ whereas it gets larger with increasing $p$.

The first and second normalized mode shapes corresponding to the first two natural frequencies for displacements $u$ and $w$ for various porosities and boundary conditions are given in Figs. 6a-d. As can be observed, mod shapes show similar variations for different porosities in the same boundary conditions. In other words, porosity does not much affect the mod shapes of free vibration.

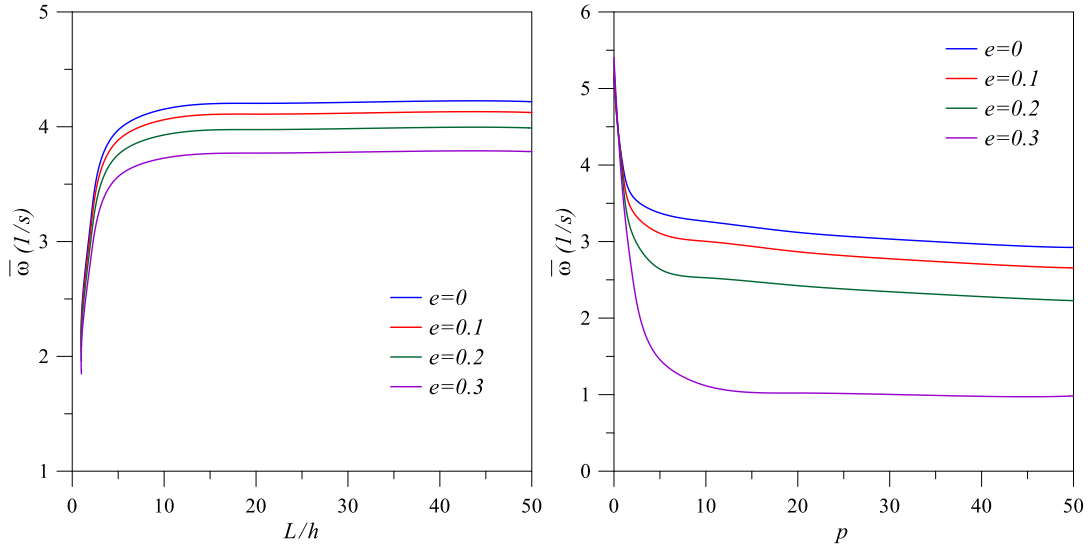


Fig. 5. The frequencies for (a) $L/h$ and (b) $p$ for various $e$ ($p = 1$ for (a), $L/h = 5$ for (b))

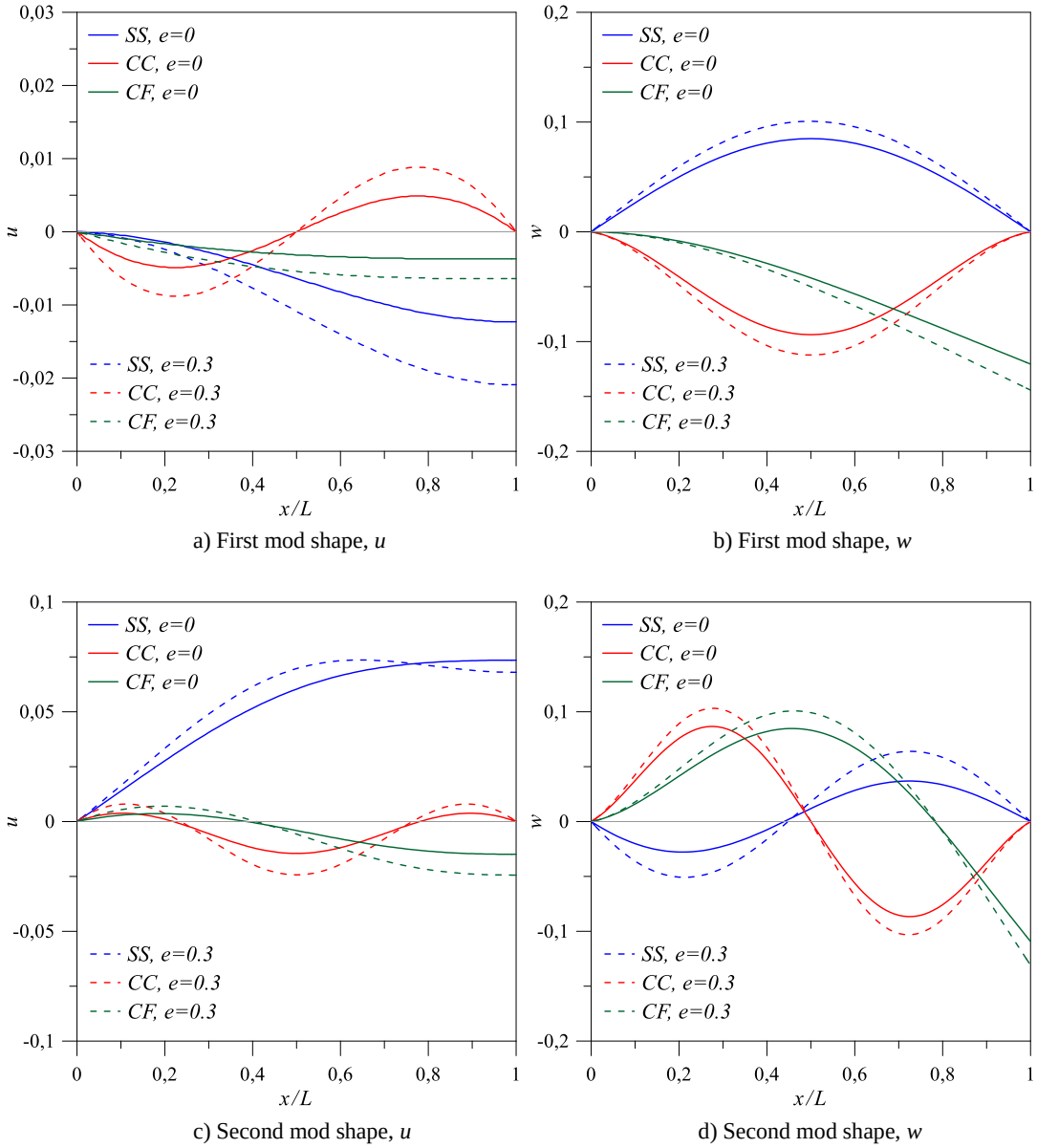


a) First mod shape, *u* b) First mod shape, *w*

c) Second mod shape, *u* d) Second mod shape, *w*

Fig. 6. The effect of *e* on the first and second mod shapes of *u* and *w* for SS, CC, and CF ($p = 1$, $L/h = 5$ )

## 4. Conclusions

In this study, the finite element analysis for the free vibration analysis of a porous FG beam is investigated using high-order shear deformation theory. A three-node 12-DOF element is used for the solution. Dimensionless neutral frequencies and mode shapes for various power law indexes, porosity index, and boundary conditions are obtained and given by tables and figures. Obtained numerical results suggest the following conclusions:

- Used finite element reflects the properties of higher-order shear deformation theory and calculates neutral frequencies close to analytical results.

- The frequencies increase if porosity at the cross-section increases for very small values of the power law index (around $p = 0$), whereas the increase of $e$ results in a decrease in frequencies for large values of $p \geq 0.5$.
- For the same porosity index, the effect of porosity on frequencies in the case of the Even type is more significant compared to the Uneven ones.
- Although the frequencies are affected due to the porosity, the mod shapes show similar characteristics.

## Declaration of conflicting interests

The author(s) declared no potential conflicts of interest with respect to the research, authorship, and/or publication of this article.

## References

[1] Karama M, Afaq KS, Mistou S (2003) Mechanical behaviour of laminated composite beam by the new multi-layered laminated composite structures model with transverse shear stress continuity. International Journal of Solids and Structures 40(6):1525-1546. https://doi.org/10.1016/S0020-7683(02)00647-9

[2] Sayyad AS, Ghugal YM (2019) Modeling and analysis of functionally graded sandwich beams: a review. Mechanics of Advanced Materials and Structures 26(21):1776-1795. https://doi.org/10.1080/15376494.2018.1447178

[3] Hadji L, Zouatnia N, Bernard F (2019) An analytical solution for bending and free vibration responses of functionally graded beams with porosities: Effect of the micromechanical models. Structural Engineering and Mechanics 69(2):231-241. https://doi.org/0.12989/sem.2019.69.2.231

[4] Kahya V, Turan M (2017) Finite element model for vibration and buckling of functionally graded beams based on the first-order shear deformation theory. Composites Part B: Engineering 109:108-115. https://doi.org/10.1016/j.compositesb.2016.10.039

[5] Nguyen T-K, Truong-Phong Nguyen T, Vo TP, Thai H-T (2015) Vibration and buckling analysis of functionally graded sandwich beams by a new higher-order shear deformation theory. Composites Part B: Engineering 76:273-285. https://doi.org/10.1016/j.compositesb.2015.02.032

[6] Vo TP, Thai H-T, Nguyen T-K, Maheri A, Lee J (2014) Finite element model for vibration and buckling of functionally graded sandwich beams based on a refined shear deformation theory. Engineering Structures 64:12-22. https://doi.org/10.1016/j.engstruct.2014.01.029

[7] Chen D, Yang J, Kitipornchai S (2015) Elastic buckling and static bending of shear deformable functionally graded porous beam. Composite Structures 133:54-61. https://doi.org/10.1016/j.compstruct.2015.07.052

[8] Wattanasakulpong N, Chaikittiratana A (2015) Flexural vibration of imperfect functionally graded beams based on Timoshenko beam theory: Chebyshev collocation method. Meccanica 50(5):1331-1342. https://doi.org/10.1007/s11012-014-0094-8

[9] Ebrahimi F, Ghasemi F, Salari E (2016) Investigating thermal effects on vibration behavior of temperature-dependent compositionally graded Euler beams with porosities. Meccanica 51(1):223-249. https://doi.org/10.1007/s11012-015-0208-y

[10] Ait Atmane H, Tounsi A, Bernard F (2017) Effect of thickness stretching and porosity on mechanical response of a functionally graded beams resting on elastic foundations. International Journal of Mechanics and Materials in Design 13(1):71-84. https://doi.org/10.1007/s10999-015-9318-x

[11] Al Rjoub YS, Hamad AG (2017) Free vibration of functionally Euler-Bernoulli and Timoshenko graded porous beams using the transfer matrix method. KSCE Journal of Civil Engineering 21(3):792-806. https://doi.org/10.1007/s12205-016-0149-6

[12] Kitipornchai S, Chen D, Yang J (2017) Free vibration and elastic buckling of functionally graded porous beams reinforced by graphene platelets. Materials & Design 116:656-665. https://doi.org/10.1016/j.matdes.2016.12.061

[13] Thi B-P, Minh Tu T, Hoang T-P, Long N (2019) Bending analysis of functionally graded beam with porosities resting on elastic foundation based on neutral surface position. Journal of Science and Technology in Civil Engineering (STCE) - NUCE 13:33-45. https://doi.org/10.31814/stce.nuce2019-13(1)-04

[14] Tang H, Li L, Hu Y (2019) Coupling effect of thickness and shear deformation on size-dependent bending of micro/nano-scale porous beams. Applied Mathematical Modelling 66:527-547. https://doi.org/10.1016/j.apm.2018.09.027

[15] Demirhan VT, Pınar A (2020) Free vibration analysis of functionally graded porous beam. 8(1):49-60 (in Turkish). https://doi.org/10.20290/estubtdb.538586

[16] Derikvand M, Farhatnia F, Hodges DH (2021) Functionally graded thick sandwich beams with porous core: Buckling analysis via differential transform method. Mechanics Based Design of Structures and Machines. https://doi.org/10.1080/15397734.2021.1931309

[17] Nguyen N-D, Nguyen T-N, Nguyen T-K, Vo TP (2022) A new two-variable shear deformation theory for bending, free vibration and buckling analysis of functionally graded porous beams. Composite Structures 282:115095. https://doi.org/10.1016/j.compstruct.2021.115095

[18] Fouda N, El-midany T, Sadoun AM (2017) Bending, buckling and vibration of a functionally graded porous beam using finite elements. Journal of Applied and Computational Mechanics 3(4):274-282. https://doi.org/10.22055/jacm.2017.21924.1121

[19] Akbaş ŞD (2018) Forced vibration analysis of functionally graded porous deep beams. Composite Structures 186:293-302. https://doi.org/10.1016/j.compstruct.2017.12.013

[20] Wu D, Liu A, Huang Y, Huang Y, Pi Y, Gao W (2018) Dynamic analysis of functionally graded porous structures through finite element analysis. Engineering Structures 165:287-301. https://doi.org/10.1016/j.engstruct.2018.03.023

[21] Wu D, Liu A, Huang Y, Huang Y, Pi Y, Gao W (2018) Mathematical programming approach for uncertain linear elastic analysis of functionally graded porous structures with interval parameters. Composites Part B: Engineering 152:282-291. https://doi.org/10.1016/j.compositesb.2018.06.032

[22] Hamed MA, Sadoun AM, Eltaher MA (2019) Effects of porosity models on static behavior of size dependent functionally graded beam. Structural Engineering and Mechanics 71(1):89-98. https://doi.org/10.12989/sem.2019.71.1.089

[23] Karamanli A, Vo TP (2021) A quasi-3D theory for functionally graded porous microbeams based on the modified strain gradient theory. Composite Structures 257:113066. https://doi.org/10.1016/j.compstruct.2020.113066

[24] Zghal S, Ataoui D, Dammak F (2022) Static bending analysis of beams made of functionally graded porous materials. Mechanics Based Design of Structures and Machines 50(3):1012-1029. https://doi.org/10.1080/15397734.2020.1748053

[25] Alnujaie A, Akbas SD, Eltaher MA, Assie AE (2021) Damped forced vibration analysis of layered functionally graded thick beams with porosity. Smart Structures and Systems 27(4):679-689. https://doi.org/10.12989/sss.2021.27.4.679